

ПН
A67/SS

VOLUME 305, 30 JUNE 2014

ISSN 0169-4332



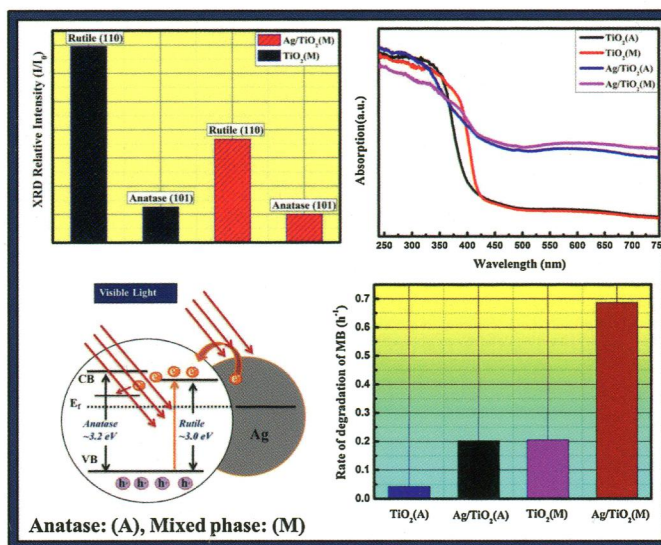
Applied Surface Science

A JOURNAL DEVOTED TO APPLIED PHYSICS
AND CHEMISTRY OF SURFACES AND INTERFACES

H. RUDOLPH EDITOR-IN-CHIEF

EDITORS

J.G. CHEN
A.R. GONZÁLEZ-ELIPE
W. HUANG
P. KINGSHOTT
H. KOBAYASHI
T. KOMEDA
T. LIPPERT
C.F. MCCONVILLE
M.F. MONTEMOR
R.L. OPILA
F. ROSEI
P. SCHAAF
A. TEPLYAKOV
R. WALLACE



applied surface science

Contents

Volume 305 (2014)

Regular Papers

- Laser-drilled micro-hole arrays on polyurethane synthetic leather for improvement of water vapor permeability
Y. Wu, A.H. Wang, R.R. Zheng, H.Q. Tang, X.Y. Qi and B. Ye 1
- Simple approach for improving gold deposition inside nanoporous alumina template on Si substrate
V.H. Nguyen, Y. Hoshi and N. Usami 9
- Laser alloying of Ti-Si compound coating on Ti-6Al-4V alloy for the improvement of bioactivity
Y. Wu, A.H. Wang, Z. Zhang, R.R. Zheng, H.B. Xia and Y.N. Wang 16
- Bioactivity and osteogenic cell response of TiO₂ nanotubes coupled with nanoscale calcium phosphate via ultrasonification-assisted electrochemical deposition
J. Chen, Z. Zhang, J. Ouyang, X. Chen, Z. Xu and X. Sun 24
- Ag deposited mixed phase titania visible light photocatalyst – Superiority of Ag-titania and mixed phase titania co-junction
A. Ramchiary and S.K. Samdarshi 33
- First-principles study of hydrogen dissociation and diffusion on transition metal-doped Mg(0 0 1) surfaces
Z. Wang, X. Guo, M. Wu, Q. Sun and Y. Jia 40
- Upgrading non-oxidized carbon nanotubes by thermally decomposed hydrazine
P.-C. Wang, Y.-C. Liao, L.-H. Liu, Y.-L. Lai, Y.-C. Lin and Y.-J. Hsu 46
- Charge defects and highly enhanced multiferroic properties in Mn and Cu co-doped BiFeO₃ thin films
G. Dong, G. Tan, Y. Luo, W. Liu, A. Xia and H. Ren 55
- Hematite nanostructuring using electrohydrodynamic lithography
F. Boudoire, R. Toth, J. Heier, A. Braun and E.C. Constable 62
- Dielectric properties and thermal destruction of poly(dimethylsiloxane)/Fe₂O₃/SiO₂ nanocomposites
M.V. Galaburda, P. Klonos, V.M. Gun'ko, V.M. Bogatyrov, M.V. Borysenko and P. Pissis 67
- Magnesium substituted hydroxyapatite coating on titanium with nanotubular TiO₂ intermediate layer via electrochemical deposition
Y. Yajing, D. Qiongqiong, H. Yong, S. Han and X. Pang 77
- Protective properties of magnetron-sputtered Ti coating on CoSb₃ thermoelectric material
D. Zhao, M. Zuo, Z. Wang, X. Teng and H. Geng 86
- The effect of ion implantation on tribology and hot rolling contact fatigue of Cr4Mo4Ni4V bearing steel
J. Jin, Y. Chen, K. Gao and X. Huang 93
- Study of nanoindentation behavior of amorphous alloy using molecular dynamics
C. Qiu, P. Zhu, F. Fang, D. Yuan and X. Shen 101
- Atomic force microscopy on phase-control pulsed force mode in water: Imaging and force analysis on a rhodium-octaethylporphyrin layer on highly oriented pyrolytic graphite
Y. Maeda, S.-i. Yamazaki and M. Kohyama 111
- Magneto-optical spectroscopy of surface/interfaces in Co/garnet heterostructures
M. Pashkevich, A. Stupakiewicz, A. Kirilyuk, A. Stognij, A. Maziewski and Th. Rasing 117
- FIM tips in SPM: Apex orientation and temperature considerations on atom transfer and diffusion
W. Paul, D. Oliver, Y. Miyahara and P. Grütter 124
- In situ study on growth behavior of interfacial bubbles and its effect on interfacial reaction during a soldering process
L. Qu, H.T. Ma, H.J. Zhao, A. Kunwar and N. Zhao 133
- Ordering of the Si(5 5 3) surface with Pb atoms
M. Kopciuszynski, P. Łukasik, R. Zdyb and M. Jałochowski 139
- Influence of deposition temperature and amorphous carbon on microstructure and oxidation resistance of magnetron sputtered nanocomposite Cr-C films
K. Nygren, M. Andersson, J. Högström, W. Fredriksson, K. Edström, L. Nyholm and U. Jansson 143
- Atomic scale structure investigations of epitaxial Fe/Cr multilayers
M. Kac, J. Morgiel, A. Polit, Y. Zabala and M. Marszałek 154
- HR-EELS study of hydrogen bonding configuration, chemical and thermal stability of detonation nanodiamond films
Sh. Michaelson, R. Akhvediani, T. Petit, H.A. Girard, J.C. Arnault and A. Hoffman 160
- Structural comparison between MgO/Fe(0 0 1) and MgO/Fe(0 0 1)-p(1 × 1)O interfaces for magnetic tunneling junctions: An Auger electron diffraction study
M. Cantoni, S. Boseggia, D. Petti, A. Cattoni and R. Bertacco 167
- Study of growth kinetics and depth resolved composition of a-SiN_x:H thin films by resonant soft X-ray reflectivity at the Si L_{2,3}-edge
R.K. Bommali, M.H. Modi, S. Zhou, S. Ghosh and P. Srivastava 173
- Electrochemical performance of ZnWO₄/CNTs composite as anode materials for lithium-ion battery
L. Zhang, Z. Wang, L. Wang, Y. Xing, X. Li and Y. Zhang 179
- Facile fabrication of hierarchical porous resins via high internal phase emulsion and polymeric porogen
L. Ma, X. Luo, N. Cai, Y. Xue, S. Zhu, Z. Fu and F. Yu 186
- Sol-gel synthesis of ZnO transparent conductive films: The role of pH
M.L. Addonizio, A. Aronne, S. Daliento, O. Tari, E. Fanelli and P. Pernice 194
- Understanding the effects of sputter damage in W-S thin films by HAXPES
J. Sundberg, R. Lindblad, M. Gorgoi, H. Rensmo, U. Jansson and A. Lindblad 203
- Enhancement of electrical characteristics and reliability in crystallized ZrO₂ gate dielectrics treated with in-situ atomic layer doping of nitrogen
J.-J. Huang, L.-T. Huang, M.-C. Tsai, M.-H. Lee and M.-J. Chen 214

(Contents continued on BM I)



(Continued from outside back cover)

- The underlying reason of DIO additive on the improvement polymer solar cells performance
Z. Wang, F. Zhang, L. Li, Q. An, J. Wang and J. Zhang 221
- An ultraviolet photodetector with an active layer composed of solution processed polyfluorene:Zn_{0.71}Cd_{0.29}S hybrid nanomaterials
S. Sevim, G. Memisoglu, C. Varlikli, L.E. Doğan, D. Tascioglu and S. Ozelcik 227
- The roles of various Ni species over SnO₂ in enhancing the photocatalytic properties for hydrogen generation under visible light irradiation
Q. Du and G. Lu 235
- Preparation and enhanced photocatalytic activity of CdS@RGO core-shell structural microspheres
H. Liu, T. Lv, X. Wu, C. Zhu and Z. Zhu 242
- Interaction of tetraethoxysilane with OH-terminated SiO₂ (0 0 1) surface: A first principles study
X. Deng, Y. Song, J. Li and Y. Pu 247
- Improved light output power of LEDs with embedded air voids structure and SiO₂ current blocking layer
S. Zhou, S. Yuan, S. Liu and H. Ding 252
- A study on high temperature oxidation behavior of double glow plasma surface metallurgy Fe-Al-Cr alloyed layer on Q235 steel
X.-X. Luo, Z.-J. Yao, P.-Z. Zhang, Q. Miao, W.-P. Liang, D.-B. Wei and Y. Chen 259
- Adsorption of environmental pollutants using magnetic hybrid nanoparticles modified with β-cyclodextrin
N. Wang, L. Zhou, J. Guo, Q. Ye, J.-M. Lin and J. Yuan 267
- Template-free facile preparation of monoclinic WO₃ nanoplates and their high photocatalytic activities
H. Zhang, J. Yang, D. Li, W. Guo, Q. Qin, L. Zhu and W. Zheng 274
- Synthesis and characterization of N-doped TiO₂ photocatalysts with tunable response to solar radiation
A. Petala, D. Tsikritzis, M. Kollia, S. Ladas, S. Kennou and D.I. Kondarides 281
- Surface modification of cellulosic substrates via atmospheric pressure plasma polymerization of acrylic acid: Structure and properties
J. Garcia-Torres, D. Sylla, L. Molina, E. Crespo, J. Mota and L. Bautista 292
- Silylation of oxidized multi-wall carbon nanotubes by catalyzed dehydrogenative cross-coupling between carboxylic and hydrosilane functions
J.-F. Seffer, S. Detriche, J. B. Nagy, J. Delhalle and Z. Mekhalif 301
- Al-Mn coating electrodeposited from ionic liquid on NdFeB magnet with high hardness and corrosion resistance
J. Ding, B. Xu and G. Ling 309
- Enhanced degradation of azo dye by nanoporous-copper-decorated Mg-Cu-Y metallic glass powder through dealloying pretreatment
X. Luo, R. Li, J. Zong, Y. Zhang, H. Li and T. Zhang 314
- Surface modification of an epoxy resin with polyamines and polydopamine: The effect on the initial electroless copper deposition
D. Schaubroeck, L. Mader, N. De Geyter, R. Morent, P. Dubruel and J. Vanfleteren 321
- Influences of the main anodic electroplating parameters on cerium oxide films
Y. Yang, Y. Yang, X. Du, Y. Chen, Z. Zhang and J. Zhang 330
- Reuse of acid coagulant-recovered drinking waterworks sludge residual to remove phosphorus from wastewater
L. Yang, J. Wei, Y. Zhang, J. Wang and D. Wang 337
- Influence of film thickness on laser ablation threshold of transparent conducting oxide thin-films
S. Rung, A. Christiansen and R. Hellmann 347
- TiO₂ hollow microspheres with mesoporous surface: Superior adsorption performance for dye removal
R. Wang, X. Cai and F. Shen 352
- Mn-doped CdS quantum dots sensitized hierarchical TiO₂ flower-rod for solar cell application
L. Yu, Z. Li, Y. Liu, F. Cheng and S. Sun 359
- A surface-chemistry study of barium ferrite nanoplates with DBSA-modified surfaces
D. Lisjak, S. Ovtar, J. Kovač, L. Gregoratti, B. Aleman, M. Amati, M. Fanetti and D. Makovec 366
- Deposition and alignment of cells on laser-patterned quartz
S.D. George, U. Ladiwala, J. Thomas, A. Bankapur, S. Chidangil and D. Mathur 375
- First-principles study of nitrobenzene adsorption on graphene
Z. Dai and Y. Zhao 382
- Preparation and characterization of silver loaded montmorillonite modified with sulfur amino acid
T. Li, O. Lin, Z. Lu, L. He and X. Wang 386
- Molecular arrangement investigation of copper phthalocyanine grown on hydrogen passivated Si(1 1 1) surfaces
I. Arbi, B. Ben Hamada, A. Souissi, S. Menzli, C. Ben Azzouz, A. Laribi, A. Akremi and C. chefi 396
- Coaxial silicon/multi-walled carbon nanotube nanocomposite anodes for long cycle life lithium-ion batteries
U. Tocoglu, O. Cevher, M.O. Guler and H. Akbulut 402
- Adsorption of copper ions by ion-imprinted simultaneous interpenetrating network hydrogel: Thermodynamics, morphology and mechanism
J. Wang, L. Ding, J. Wei and F. Liu 412
- Optimal processing for hydrophobic nanopillar polymer surfaces using nanoporous alumina template
C.F. Huang, Y. Lin, Y.K. Shen and Y.M. Fan 419
- Synthesis and characterization of LiFePO₄ electrode materials coated by graphene
Z. Tian, S. Liu, F. Ye, S. Yao, Z. Zhou and S. Wang 427
- Porous CoO nanostructures grown on three-dimension graphene foams for supercapacitors electrodes
W. Deng, W. Lan, Y. Sun, Q. Su and E. Xie 433
- 18.5% efficient AlO_x/SiN_y rear passivated industrial multicrystalline silicon solar cells
Q. Qiao, H. Lu, J. Ge, X. Xi, R. Chen, J. Yang, J. Zhu, Z. Shi and J. Chu 439
- A high-sensitivity, fast-response, rapid-recovery p-n heterojunction photodiode based on rutile TiO₂ nanorod array on p-Si(1 1 1)
A.M. Selman, Z. Hassan, M. Husham and N.M. Ahmed 445
- Transient variation of a cross-sectional area of inkjet-printed silver nanoparticle ink during furnace sintering
D. Kim, I. Lee, Y. Yoo, Y.-J. Moon and S.-J. Moon 453
- In situ* synthesis of CdS decorated titanate nanosheets with highly efficient visible-light-induced photoactivity
Z. Liu, P. Fang, F. Liu, Y. Zhang, X. Liu, D. Lu, D. Li and S. Wang 459
- Surface roughness and electrical resistivity of high-purity zinc irradiated with nanosecond visible laser pulses
M.Z. Butt, D. Ali, M.U. Tanveer and S. Naseem 466

Fabrication and electrical characterization of Li–N dual doped ZnO thin film transistor D.Z. Zhou, B. Li, H.L. Wang, M. Salik, H.H. Wu, Z.F. Hu, S. Gao, Y.F. Peng, L.X. Yi, X.Q. Zhang and Y.S. Wang	474	Study of material removal processes of the crystal silicon substrate covered by an oxide film under a silica cluster impact: Molecular dynamics simulation R. Chen, Y. Wu, H. Lei, R. Jiang and M. Liang	609
The dependence of Zn content on thermal treatments for Cd _{1-x} Zn _x Te thin films deposited by close-spaced sublimation H. Xu, R. Xu, J. Huang, J. Zhang, K. Tang and L. Wang	477	Potassium-doped copper oxide nanoparticles synthesized by a solvothermal method as an anode material for high-performance lithium ion secondary battery T.V. Thi, A.K. Rai, J. Gim and J. Kim	617
A study on Ti-doped ZnO transparent conducting thin films fabricated by pulsed laser deposition W. Zhao, Q. Zhou, X. Zhang and X. Wu	481	Nanosheet based SnO ₂ assemblies grown on a flexible substrate S. Zhang, B. Yin, Y. Jiao, Y. Liu, F. Qu and X. Wu	626
Physical mechanisms of macroparticles number density decreasing on a substrate immersed in vacuum arc plasma at negative high-frequency short-pulsed biasing A.I. Ryabchikov, D.O. Sivin and A.I. Bumagina	487	Improved mechanical performance of PBO fiber-reinforced bismaleimide composite using mixed O ₂ /Ar plasma D. Liu, P. Chen, Q. Yu, K. Ma and Z. Ding	630
The use of trivalent chromium bath to obtain a solar selective black chromium coating S. Survilienė, A. Češūnienė, R. Juškėnas, A. Selskienė, D. Bučinskienė, P. Kalinauskas, K. Juškevičius, I. Jurevičiūtė	492	Improved efficiency and stability of GaN photoanode in photoelectrochemical water splitting by NiO cocatalyst S.H. Kim, M. Ebaid, J.-H. Kang and S.-W. Ryu	638
Corrosion resistance and long-term durability of super-hydrophobic nickel film prepared by electrodeposition process S. Khorsand, K. Raeissi and F. Ashrafzadeh	498	Redox properties and metal-support interaction of Pd/Ce _{0.67} Zr _{0.33} O ₂ -Al ₂ O ₃ catalyst for CO, HC and NO _x elimination S. Lin, L. Yang, X. Yang and R. Zhou	642
XPS analysis and structural and morphological characterization of Cu ₂ ZnSnS ₄ thin films grown by sequential evaporation G. Gordillo, C. Calderón and P. Bartolo-Pérez	506	Analysis of nanopore arrangement of porous alumina layers formed by anodizing in oxalic acid at relatively high temperatures L. Zaraska, W.J. Stepniowski, M. Jaskała and G.D. Sulka	650
Antimicrobial mechanism of flavonoids against <i>Escherichia coli</i> ATCC 25922 by model membrane study M. He, T. Wu, S. Pan and X. Xu	515	Role of electroless nickel diffusion barrier on the combinatorial plating characteristics of dense Pd/Ni/PSS composite membranes M. Pujari, A. Agarwal, R. Uppaluri and A. Verma	658
Optimization and characterization of biomolecule immobilization on silicon substrates using (3-aminopropyl)triethoxysilane (APTES) and glutaraldehyde linker N.S.K. Gunda, M. Singh, L. Norman, K. Kaur and S.K. Mitra	522	Hydrogen production by photocatalytic ethanol reforming using Eu- and S-doped anatase J. Puskelova, R. Michal, M. Caplovicova, M. Antoniadou, L. Caplovic, G. Plesch and P. Lianos	665
High dielectric constant and low dielectric loss hybrid nanocomposites fabricated with ferroelectric polymer matrix and BaTiO ₃ nanofibers modified with perfluoroalkylsilane X. Zhang, Y. Ma, C. Zhao and W. Yang	531	Cross-sectional study of high spatial frequency ripples performed on silicon using nanojoule femtosecond laser pulses at high repetition rate R. Le Harzic, M. Menzel, S. Henning, A. Heilmann, F. Stracke and H. Zimmermann	670
Amorphous carbon enhancement of hydrogen penetration into UO ₂ S. Zalkind, N. Shamir, T. Gouder, R. Akhvediani and A. Hoffman	539	Oxidation of Inconel 625 superalloy upon treatment with oxygen or hydrogen plasma at high temperature A. Vesel, A. Drenik, K. Elersic, M. Mozetic, J. Kovac, T. Gyergyek, J. Stockel, J. Varju, R. Panek and M. Balat-Pichelin	674
Passivation of the La ₂ NiMnO ₆ double perovskite to hydroxylation by excess nickel, and the fate of the hydroxylated surface upon heating A.T. Fulmer, J. Dondlinger and M.A. Langell	544	One-step synthesis Fe ₃ N surface-modified Fe ₃ O ₄ nanoparticles with excellent lithium storage ability Y. Li, Y. Yan, H. Ming and J. Zheng	683
Hydrophobicity enhancement of Al ₂ O ₃ thin films deposited on polymeric substrates by atomic layer deposition with perfluoropropane plasma treatment K. Ali, K.-H. Choi, C.Y. Kim, Y.H. Doh and J. Jo	554	Temperature driven three-dimensional ordering of InGaAs/GaAs quantum dot superlattices grown under As ₂ gas flux P.M. Lytvyn, Yu.I. Mazur, M. Benamara, M.E. Ware, V.G. Dorogan, L.D. de Souza, E. Marega Jr., M.D. Teodoro, G.E. Marques and G.J. Salamo	689
Uniform TiO ₂ -SiO ₂ hollow nanospheres: Synthesis, characterization and enhanced adsorption-photodegradation of azo dyes and phenol N. Guo, Y. Liang, S. Lan, L. Liu, G. Ji, S. Gan, H. Zou and X. Xu	562	Hafnium carbide nanocrystal chains for field emitters S. Tian, H. Li, Y. Zhang, J. Ren, X. Qiang and S. Zhang	697
Localized dispersing of ceramic particles in tool steel surfaces by pulsed laser radiation K. Hilgenberg, K. Behler and K. Steinhoff	575	Robust superhydrophobic transparent coatings fabricated by a low-temperature sol-gel process W.-H. Huang and C.-S. Lin	702
Cyclodextrin-grafted electrospun cellulose acetate nanofibers via "Click" reaction for removal of phenanthrene A. Celebioglu, S. Demirci and T. Uyar	581	Growth of Cu ₂ O flower/grass-like nanoarchitectures and their photovoltaic effects L. Hu, Y. Ju, M. Chen, A. Hosoi and S. Arai	710
Reducing ice adhesion by hierarchical micro-nano-pillars Y. He, C. Jiang, X. Cao, J. Chen, W. Tian and W. Yuan	589	A fast method to fabricate superhydrophobic surfaces on zinc substrate with ion assisted chemical etching Y. Qi, Z. Cui, B. Liang, R.S. Parnas and H. Lu	716
Carbon and functionalized graphene oxide coated vanadium oxide electrodes for lithium ion batteries V.S. Reddy Channu, D. Ravichandran, B. Rambabu and R. Holze	596	Synthesis and characterization of alkylamine-functionalized graphene for polyolefin-based nanocomposites X. Yang, T. Mei, J. Yang, C. Zhang, M. Lv and X. Wang	725
Superhydrophobic membranes on metal substrate and their corrosion protection in different corrosive media N. Wang and D. Xiong	603		

Structural and morphology analysis of annealed $Y_3(Al,Ga)_5O_{12}:Tb$ thin films synthesized by pulsed laser deposition A. Yousif, H.C. Swart, J.J. Terblans, R.M. Jafer, V. Kumar, R.E. Kroon, O.M. Ntwaeaborwa and M.M. Duvenhage	732	Superhydrophobic coating deposited directly on aluminum A.M. Escobar and N. Llorca-Isern	774
Preparation of nanostructured PbS thin films as sensing element for NO_2 gas S. Kaci, A. Keffous, S. Hakoum, M. Trari, O. Mansri and H. Menari	740	Antibacterial kaolinite/urea/chlorhexidine nanocomposites: Experiment and molecular modelling S. Holešová, M. Valášková, D. Hlaváč, J. Madejová, M. Samlíková, J. Tokarský and E. Pazdziora	783
Beta-cyclodextrins conjugated magnetic Fe_3O_4 colloidal nanoclusters for the loading and release of hydrophobic molecule S. Lv, Y. Song, Y. Song, Z. Zhao and C. Cheng	747	Adhesion of TiO_2 nanotube arrays on transparent conducting substrates using CNT- TiO_2 composite pastes C.B. Song, Y.H. Qiang, Y.L. Zhao, X.Q. Gu, D.M. Song and L. Zhu	792
Preparation and photocatalytic activity of $Mg_xZn_{1-x}O$ thin films on silicon substrate through sol-gel process C. Liu, F. Shang, G. Pan, F. Wang, Z. Zhou, W. Gong, Z. Zi, Y. Wei, X. Chen, J. Lv, G. He, M. Zhang, X. Song and Z. Sun	753	Nano crystalline high energy milled 5083 Al powder deposited using cold spray M.R. Rokni, C.A. Widener, A.T. Nardi and V.K. Champagne	797
Controlling particle size and photoelectrochemical properties of nanostructured WO_3 with surfactants A. Memar, C.M. Phan and M.O. Tade	760	Characterization of Ta-Si-N coatings prepared using direct current magnetron co-sputtering Y.-I. Chen, K.-Y. Lin, H.-H. Wang and Y.-R. Cheng	805
Long-range ferromagnetic graphene via compensated Fe/ NO_2 co-doping R. Zhang, Y. Luo, S. Qi and X. Xu	768	Surface oxidation phenomenon and mechanism of AISI 304 stainless steel induced by Nd:YAG pulsed laser C.Y. Cui, X.G. Cui, X.D. Ren, M.J. Qi, J.D. Hu and Y.M. Wang	817